

THE NATURE OF HYPERVELOCITY STARS AND THE TIME BETWEEN THEIR FORMATION AND EJECTION

WARREN R. BROWN¹, JUDITH G. COHEN², MARGARET J. GELLER¹, AND SCOTT J. KENYON¹

¹Smithsonian Astrophysical Observatory, 60 Garden St, Cambridge, MA 02138

²Palomar Observatory, Mail Stop 249-17, California Institute of Technology, Pasadena, CA 91125

Accepted in ApJ Letters

ABSTRACT

We obtain Keck HIRES spectroscopy of HVS5, one of the fastest unbound stars in the Milky Way halo. We show that HVS5 is a $3.62 \pm 0.11 M_{\odot}$ main sequence B star at a distance of 50 ± 5 kpc. The difference between its age and its flight time from the Galactic center is $105 \pm 18(\text{stat}) \pm 30(\text{sys})$ Myr; flight times from locations elsewhere in the Galactic disk are similar. This 10^8 yr ‘arrival time’ between formation and ejection is difficult to reconcile with any ejection scenario involving massive stars that live for only 10^7 yr. For comparison, we derive arrival times of 10^7 yr for two unbound runaway B stars, consistent with their disk origin where ejection results from a supernova in a binary system or dynamical interactions between massive stars in a dense star cluster. For HVS5, ejection during the first 10^7 yr of its lifetime is ruled out at the $3\text{-}\sigma$ level. Together with the 10^8 yr arrival times inferred for three other well-studied hypervelocity stars, these results are consistent with a Galactic center origin for the HVSs. If the HVSs were indeed ejected by the central black hole, then the Galactic center was forming stars $\simeq 200$ Myr ago, and the progenitors of the HVSs took $\simeq 100$ Myr to enter the black hole’s loss cone.

Subject headings: Galaxy: halo — Galaxy: center — Galaxy: kinematics and dynamics — stars: early-type — stars: individual (SDSS J091759.47+672238.35)

1. INTRODUCTION

Hills (1988) first predicted unbound “hypervelocity” stars (HVSs) as the inevitable consequence of 3-body interactions close to the tidal radius of a massive black hole. There is overwhelming evidence for a $4 \times 10^6 M_{\odot}$ central black hole in the Milky Way (Ghez et al. 2008; Gillessen et al. 2009). Theorists expect that the black hole ejects $\sim 10^{-4}$ HVSs yr⁻¹ (e.g. Perets et al. 2007), which means there are thousands of HVSs in the outer halo. Brown et al. (2005) discovered the first HVS, a luminous B-type star traveling twice the Galactic escape velocity at a distance of $\simeq 100$ kpc, and Brown et al. (2012) have subsequently discovered 15 more unbound B-type stars in their targeted HVS survey. Establishing the evolutionary state of the HVSs is important for establishing their ages, distances, and flight times. We define the difference between a HVS’s age and its flight time as the ‘arrival time’ (t_{arr}), the time between its formation and ejection. In this paper we derive t_{arr} for both HVSs and unbound runaway stars.

The arrival time provides a useful discriminant between proposed ejection mechanisms. If HVSs are ejected in three-body interactions with the Milky Way’s central black hole (Hills 1988), then the arrival times reflect the timescale for HVSs to achieve orbits that interact with the central black hole. For HVSs formed in the central region of the Galaxy, we expect $t_{\text{arr}} = 0.1\text{--}1$ Gyr (Merritt & Poon 2004; Wang & Merritt 2004). On the other hand, in both mechanisms for ejecting runaway stars from the Galactic disk – a supernova in a binary system or a dynamical interaction among massive stars in a dense star cluster – a maximum $t_{\text{arr}} \approx 10$ Myr is set by the main sequence lifetime of $\gtrsim 10 M_{\odot}$ stars. Thus, measuring t_{arr} for an ensemble of HVSs should distin-

guish between a Galactic center or Galactic disk origin.

The evolutionary state of most known HVSs (Brown et al. 2012) is ambiguous because their effective temperatures and surface gravities are consistent with both old, evolved stars (blue horizontal branch stars) and short-lived main sequence stars. Thus we must turn to other measures to establish their nature. Metallicity is one possibility; we expect that recently formed stars should have solar or super-solar metallicities. Metallicity is inconclusive, however, given the observed metallicity distribution function of stars in the Milky Way.

Projected stellar rotation $v \sin i$ is a better discriminant between evolved stars and main sequence stars. Blue horizontal branch stars have evolved through the giant branch phase and have median $v \sin i = 9$ km s⁻¹; the most extreme blue horizontal branch star rotates at 40 km s⁻¹ (Behr 2003). Late B-type main sequence stars, on the other hand, have median $v \sin i = 150$ km s⁻¹; the most extreme objects rotate at ≥ 350 km s⁻¹ (Abt et al. 2002; Huang & Gies 2006). Löckmann & Baumgardt (2008) argue that HVSs may be spun-up by a binary black hole ejection, but there is presently no evidence for a binary black hole in the Galactic center. Close binaries that produce HVSs and runaways in the Milky Way may exhibit slower stellar rotation because of tidal synchronization; Hansen (2007) predicts that late B-type HVSs ejected by the Hills mechanism should have $v \sin i = 70\text{--}90$ km s⁻¹. In any case, fast rotation is the signature of a main sequence star.

Of the B-type HVSs discovered to date, only HVS3, HVS7, and HVS8 have been studied with high-resolution spectroscopy. In all cases they are main sequence B stars with $55 < v \sin i < 260$ km s⁻¹ (Edelmann et al. 2005; Przybilla et al. 2008b; Bonanos et al. 2008; López-Morales & Bonanos 2008;

Przybilla et al. 2008c). Moderate-dispersion spectroscopy of HVS1 suggests it has $v \sin i = 190 \text{ km s}^{-1}$ (Heber et al. 2008b), another short-lived B star.

Here, we describe high resolution spectroscopy of HVS5, a $g = 17.9$ mag star located at declination $+67^\circ$ accessible only with Keck HIRES. HVS5 is a rapidly rotating $3.6 M_\odot$ main sequence B star. The difference between its age and its flight time from the Milky Way is $105 \pm 18(\text{stat}) \pm 30(\text{sys})$ Myr, inconsistent with ejection models involving massive stars.

In Section 2 we describe the observations and stellar atmosphere analysis. In Section 3 we discuss the arrival times for the HVSs and unbound disk runaways. We conclude in Section 4.

2. DATA

2.1. Observations

We observed HVS5 using the HIRES spectrograph (Vogt et al. 1994) at the 10 m Keck 1 telescope, obtaining four 1800 sec exposures the night of 2012 Jan 29, and five more the following night. Both nights were clear with 0.7–0.8 arcsec seeing. The red HIRES collimator was used in an instrument configuration that gave spectral coverage from 3920 to 8350 Å. A 1.1 arcsec slit gives a spectral resolution of $R = 34,000$, with 6.7 pixels per spectral resolution element. There are small gaps between the three CCDs that form the detector mosaic, sometimes resulting in the loss of all or part of a single echelle order.

We also observed eight B stars selected from Abt et al. (2002) that span a wide range in luminosity class (I, III, and V) and a large range in projected rotational velocity ($5 < v \sin i < 285 \text{ km s}^{-1}$). The stars are HR1328, HR1333, HR1399, HR1419, HR1420, HR1462, HR1573, HR1595, and HR1640. We used high S/N spectra of these eight B stars to provide a comparison for HVS5 and to validate our analysis below.

We used the pipeline package MAKEE¹ to remove the instrumental signature, extract a one dimensional spectrum for each echelle order, and calibrate the wavelength scale from Th-A arc spectra taken at the beginning and end of each night. Each exposure of HVS5 was individually processed through MAKEE, and the results summed. With a total integration of 4.5 hours, we achieved a S/N ratio of 70 per spectral resolution element at 4500 Å.

2.2. Spectral Analysis

Visual inspection reveals that HVS5 is a fast rotator. The full width at half maximum of the Mg II $\lambda 4481$ line compared with the Abt et al. (2002) B stars suggests a projected rotation velocity of $\simeq 130 \text{ km s}^{-1}$. We turn to the most recent ATLAS9 model atmosphere grids (Castelli & Kurucz 2004; Castelli et al. 1997) to perform a more quantitative analysis. We use the program SPECTRUM (Gray & Corbally 1994) to calculate synthetic spectra under the assumption of plane-parallel atmosphere and local thermodynamic equilibrium. We adopt macro- and microturbulence velocities of 0 and 2 km s^{-1} , respectively. All synthetic spectra are smoothed to a res-

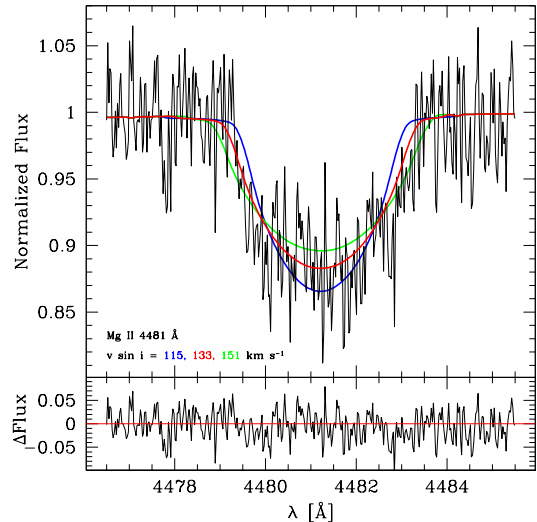


FIG. 1.— Observed Mg II $\lambda 4481$ Å line (upper panel) and its residuals (lower panel) compared to the best-fit $v \sin i = 133 \pm 7 \text{ km s}^{-1}$ model (red line). For reference, the green and blue lines are the $\pm 3\text{-}\sigma$ models.

olution of $R = 34,000$ and re-sampled with spline interpolation to match the sampling of the observed spectra.

Our approach is to analyze the spectral lines on an order-by-order basis. We normalize the continuum, calculate the χ^2 of each synthetic model against the data, and then fit the resulting distribution of χ^2 to derive the best-fitting parameters. Uncertainty estimates are provided by a standard $\Delta\chi^2$ offset to the minimum χ^2 (Press et al. 1992). Our final values are the weighted means and error-on-the-means of the parameters measured from lines in different orders.

We begin by using all of the spectral lines to solve for the heliocentric radial velocity. The best-fit $+552 \pm 3 \text{ km s}^{-1}$ velocity is in perfect agreement with the $+553 \pm 9 \text{ km s}^{-1}$ velocity measured from medium-resolution spectroscopy at the MMT (Brown et al. 2012). The constancy in velocity is consistent with HVS5 being a single star, as one expects for the product of a binary disruption. The radial velocity corresponds to a minimum velocity of $+663 \text{ km s}^{-1}$ in the Galactic rest frame (see Brown et al. 2012).

Next, we measure projected rotation using Mg II $\lambda 4481$ Å, the strongest metal line in the spectrum (see Figure 1). The best-fit $v \sin i$ is $133 \pm 7 \text{ km s}^{-1}$. For comparison, Figure 1 plots the $\pm 3\text{-}\sigma$ values as well as the residuals to the best-fit $v \sin i$. The observed $v \sin i$ is consistent with the median $v \sin i$ of comparable B-type main sequence stars (Abt et al. 2002; Huang & Gies 2006).

Given the observed $v \sin i$, we measure effective temperature and surface gravity by fitting the widths and depths of the T_{eff} - and $\log g$ -sensitive hydrogen Balmer lines. We note that the model hydrogen lines are computed using the D. Peterson routine adopted by SYNTHETIC (Kurucz 1993), which includes Stark and resonance broadening and fine structure in the cores. The best-fit values are $T_{\text{eff}} = 12,000 \pm 350 \text{ K}$ and $\log g = 3.89 \pm 0.13$; Figure 2 compares the best-fit model with the data.

Finally, we attempt to constrain the metallicity. Because of the large $v \sin i$, Fe lines are faint continuum

¹ MAKEE was developed by T.A. Barlow specifically for reduction of Keck HIRES data. It is freely available from the Keck HIRES home page www2.keck.hawaii.edu/inst/hires.

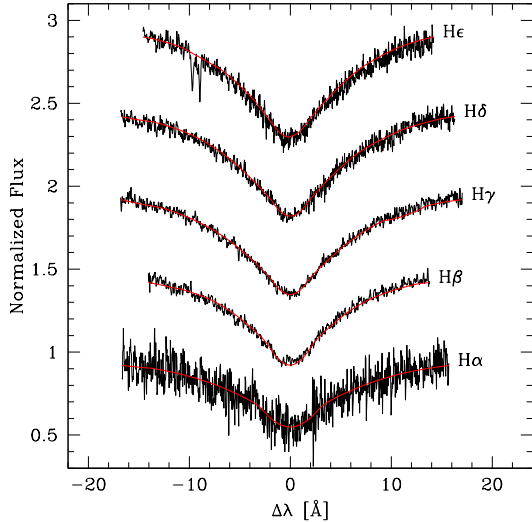


FIG. 2.— Observed hydrogen Balmer lines compared to the best-fit model (red line). The temperature- and surface gravity-sensitive lines give best-fit values of $T_{\text{eff}} = 12,000 \pm 350$ K and $\log g = 3.89 \pm 0.13$.

fluctuations and are thus too weak to provide significant constraint. Si II lines at $\lambda 4128$, $\lambda 4131$, and $\lambda 5056$ Å are stronger and yield a best-fit Si abundance of $[M/H] = -0.4 \pm 0.5$. The Mg II $\lambda 4481$ Å line (see Figure 1), on the other hand, yields a best-fit Mg abundance of $[M/H] = +0.3 \pm 0.5$. Given the large uncertainties, we conclude that HVS5 is consistent with solar abundance.

Figure 3 compares the measured T_{eff} and $\log g$ with the latest Girardi et al. (2002, 2004) solar metallicity main sequence tracks. The ellipse in Figure 3 is the 68.3% ($1-\sigma$) confidence region. Interpolating the tracks indicates that HVS5 is a $3.62 \pm 0.11 M_{\odot}$ star. As an illustration of the systematic uncertainty, we derive $3.58 M_{\odot}$ from Ekström et al. (2012) tracks with rotation, and $3.72 M_{\odot}$ from Girardi et al. (2002, 2004) +0.2 dex super-solar tracks. These values are consistent within our $1-\sigma$ uncertainty, thus the inferred mass is relatively insensitive to rotation and metallicity.

Table 1 summarizes our stellar parameters for HVS5. We also list the parameters for HVS7, HVS8, and HVS1 measured by Przybilla et al. (2008c), López-Morales & Bonanos (2008), and Heber et al. (2008b), respectively. HVS3, a probable blue straggler (Brown et al. 2010), is not directly comparable and is not included in our discussion.

3. DISCUSSION

3.1. Hypervelocity Star Flight Times and Ages

We use the Girardi et al. (2002, 2004) tracks to derive age and luminosity from the measured T_{eff} and $\log g$. We note that the $T_{\text{eff}}-\log g$ error ellipse becomes a banana shape in the age- M_g plot (Figure 4) because of the time evolution of these parameters. Interpolating the tracks indicates that HVS5 has an age of 170 ± 17 Myr and an absolute magnitude of $M_g = -0.65 \pm 0.19$.

Knowing the luminosity of HVS5, we can calculate its distance and flight time. HVS5 has an apparent dereddened magnitude of $g = 17.557 \pm 0.021$ and thus a heliocentric distance of 44 ± 4 kpc. Assuming the Sun is located 8 kpc from the Galactic center, HVS5 has a

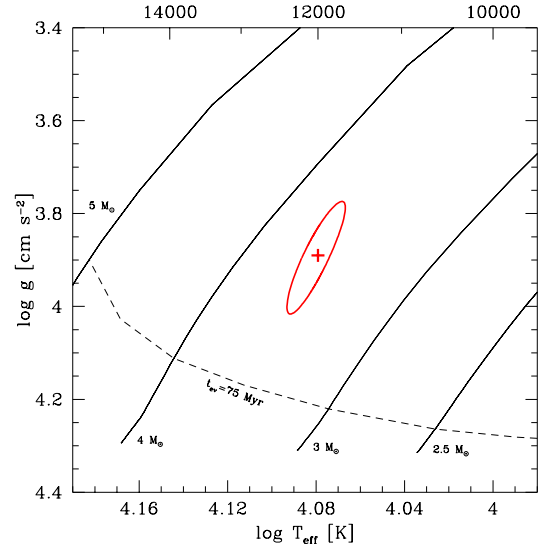


FIG. 3.— Measured T_{eff} , $\log g$ and the $1-\sigma$ error ellipse for HVS5 (in red) compared to Girardi et al. (2002, 2004) solar metallicity main sequence tracks for $2.5-5 M_{\odot}$ stars (solid black lines); the $t_{\text{ev}} = 75$ Myr isochrone is plotted for reference. HVS5 is a $3.62 \pm 0.11 M_{\odot}$ star.

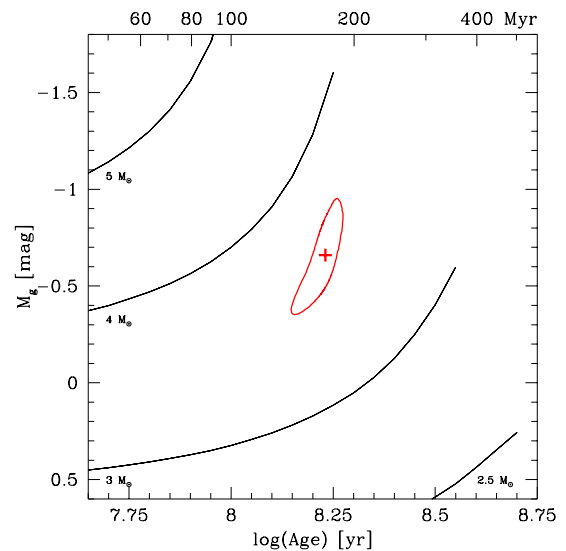


FIG. 4.— Same tracks as Figure 3 but now plotting age versus absolute magnitude. HVS5 has a formal age of $170 \pm 17(\text{stat}) \pm 30(\text{sys})$ Myr.

Galactocentric distance of $r_{GC} = 50 \pm 5$ kpc. We then take the Galactic potential model of Kenyon et al. (2008) and calculate all possible trajectories that HVS5 could have given its present distance and radial velocity. The trajectory that passes through the Galactic center has a flight time of $t_{GC} = 65 \pm 7$ Myr. The error comes from propagating the distance and radial velocity errors through the trajectory calculation.

Our Galactic center flight time estimate is appropriate for a wide range of Milky Way starting locations because HVS5 is located at high Galactic latitude and at large distance. Moving the assumed starting location of HVS5 from $r_{GC} = 0$ kpc to $r_{GC} = 10$ kpc changes the flight times by ± 8.5 Myr, which is similar to the estimated uncertainty in flight time.

TABLE 1
HYPERVELOCITY STAR PROPERTIES

	HVS5	HVS7	HVS8	HVS1
T_{eff} (K)	12000 ± 350	12000 ± 500	11000 ± 1000	11000 ± 500
$\log g$ (cgs)	3.89 ± 0.13	3.8 ± 0.1	3.75 ± 0.25	3.74 ± 0.20
$v \sin i$ (km s $^{-1}$)	133 ± 7	55 ± 2	260 ± 70	190 ± 40
Mass (M_{\odot})	3.62 ± 0.11	3.79 ± 0.09	3.49 ± 0.22	3.50 ± 0.18
Age (Myr)	170 ± 17	170 ± 15	220 ± 25	220 ± 20
M_g (mag)	-0.65 ± 0.19	-0.94 ± 0.14	-0.77 ± 0.35	-0.80 ± 0.29
g_0 (mag)	17.557 ± 0.021	17.637 ± 0.019	17.939 ± 0.016	19.688 ± 0.023
r_{GC} (kpc)	50 ± 5	53 ± 4	60 ± 10	130 ± 18
t_{GC} (Myr)	65 ± 7	105 ± 10	120 ± 20	175 ± 25
$t_{\text{arr}} = \text{Age} - t_{GC}$ (Myr)	105 ± 18	65 ± 18	100 ± 32	45 ± 32

For self-consistency, we also derive the ages and flight times of HVS7, HVS8, and HVS1 using the same tracks and methodology. Table 1 summarizes the derived values. The HVSs have ages of 170–220 Myr and flight times of 45–175 Myr.

3.2. Links to Unbound Ejection Processes

There are many ways to eject stars from their place of origin, but few processes can accelerate stars to unbound velocities. Because most B stars are binaries (e.g. Chini et al. 2012), disk “runaway” B stars are explained by binary disruption mechanisms. In the case of a supernova in a binary system, the timescale of the process is the lifetime of the $\gtrsim 10 M_{\odot}$ star that explodes, 10^6 – 10^7 yr. In the case of dynamical 3- and 4-body encounters, e.g. in young star clusters, massive stars are necessary to attain the unbound velocities of HVSs and thus the timescale of the dynamical process is also $\simeq 10^7$ yr. Except in rare circumstances (Gualandris & Portegies Zwart 2007; Gvaramadze et al. 2009; Silva & Napiwotzki 2011), no runaway mechanism is expected to yield unbound velocities for $3 M_{\odot}$ stars (Portegies Zwart 2000; Perets & Subr 2012).

A more energetic and higher ejection rate process exists in the Galactic center: HVSs ejected by the central black hole (Hills 1988). The B stars that presently orbit Sgr A* on short-period, eccentric orbits are, in this scenario, the former companions of HVSs; their progenitors are believed to have formed further out and then moved in towards the black hole through dynamical processes (e.g. Perets et al. 2007, 2009; Madigan et al. 2009, 2011).

In principle, there is no upper limit to the arrival time t_{arr} for the central black hole ejection process. The black hole is always there, and on-going star formation (e.g. Lu et al. 2009) provides a constant supply of new stars. To derive a typical t_{arr} , we consider the ‘loss cone,’ the set of orbits which have a distance of closest approach within the black hole’s tidal radius. For an ensemble of stars formed close to the black hole, a few will have orbits that interact with the black hole on $\lesssim 1$ Myr timescales and so are quickly removed. As a result of dynamical interactions with other massive objects or the long-term evolution of chaotic orbits within a triaxial potential, the remaining stars will ‘fill’ the loss cone with timescales of 100 Myr to 1 Gyr (Yu & Tremaine 2003; Merritt & Poon 2004; Wang & Merritt 2004; Perets et al. 2007).

Timescale thus provides an important distinction between the central black hole and disk runaway ejection processes. The disk runaway scenarios must eject stars

within the 1–10 Myr lifetimes of massive stars to attain unbound velocities. The central black hole can eject unbound stars at any time, however we expect that stars formed in the Galactic center will have typical arrival times of 0.1–1 Gyr. For the HVSs studied here, an upper limit is provided by their finite lifetimes.

3.3. Comparison with Observations

From Table 1, observed HVSs have $t_{\text{arr}} \approx 50$ – 100 Myr. The formal error in t_{arr} is likely an underestimate of the true error, however. Perhaps the best estimate of systematic error comes from comparing the measured stellar parameters with different sets of stellar evolution tracks. For HVS5, the Ekström et al. (2012) tracks for rotating stars give a longer age of 200 ± 23 Myr, while the Girardi et al. (2002, 2004) +0.2 dex super-solar tracks give a shorter age of 142 ± 16 Myr. Taking the ± 30 Myr age spread as the systematic error rules out an ejection in the first 10 Myr of HVS5’s lifetime at the $3\text{-}\sigma$ level. This confidence level is corroborated by the directly measured parameters: the $\log g$ and T_{eff} of a 75 Myr old $3.62 M_{\odot}$ star differ by $2.1\text{-}\sigma$ and $3.3\text{-}\sigma$, respectively, with respect to HVS5’s present values (see Figure 3). Thus for HVS5 we rule out a possible $t_{\text{arr}} \lesssim 10$ Myr at the $3\text{-}\sigma$ level, an interesting and important constraint on its origin.

The hyper-runaways first discovered by Heber et al. (2008a) show a contrasting result. HD 271791 is an unbound $11 M_{\odot}$ B star. The observed proper motion shows it was ejected in the direction of rotation from the outer disk (Heber et al. 2008a). The star has an age of 25 ± 5 Myr and a flight time from the disk of 25 ± 6 Myr. Formally, the star has $t_{\text{arr}} = 0 \pm 8$ Myr. The marginally unbound $5 M_{\odot}$ B star HIP 60350 is similar (Irrgang et al. 2010). It has an age of 45^{+15}_{-30} Myr and a flight time from the disk of 14 ± 3 Myr. Thus, $t_{\text{arr}} = 31^{+15}_{-30}$ Myr. The short arrival times are consistent with both the supernova ejection scenario (Przybilla et al. 2008a) and the dynamical ejection scenario (Gvaramadze 2009). Contrasting the derived arrival times with arrival times for HVSs underscores the usefulness of t_{arr} as a model discriminant.

Other objects are more ambiguous. Tillich et al. (2009) discovered the marginally unbound $2.5 M_{\odot}$ A star J0136+2425 with a derived age of 245 Myr and a flight time of 12 Myr if it comes from the disk. Accepting modern Milky Way halo mass estimates of $\simeq 1.7 \times 10^{12} M_{\odot}$ (e.g. Gnedin et al. 2010; Przybilla et al. 2010), it is bound to the Milky Way and may be explained as a halo star. The evolved sdB star J1211+1437 has a flight time that is also a small fraction of its progen-

itor's lifetime (which may be many Gyr) (Tillich et al. 2011). Given the $\pm 140 \text{ km s}^{-1}$ uncertainty in the space motion, this sdB star is also consistent with being bound and thus a normal halo star.

The HVSs are significantly unbound based on radial velocity alone. The four HVSs with known evolutionary state discussed here have $t_{\text{arr}} = 50\text{--}100 \text{ Myr}$, times both larger than known hyper-runaways and larger than the maximum t_{arr} expected in the mechanisms for producing hyper-runaways. However, their t_{arr} are close to the arrival times expected for dynamical interactions with the black hole at the Galactic center.

4. CONCLUSION

We describe Keck HIRES spectroscopy of HVS5, one of the fastest known HVSs with a minimum Galactic rest frame velocity of $+663 \pm 3 \text{ km s}^{-1}$. The observations reveal that HVS5 has a projected rotation of $v \sin i = 133 \pm 7 \text{ km s}^{-1}$ and is thus a main sequence B star. Comparing the measured T_{eff} and $\log g$ with stellar evolution tracks indicates that HVS5 is a $3.62 \pm 0.11 M_{\odot}$, $170 \pm 17 \text{ Myr}$ old star. Given its present distance and radial velocity, we calculate that HVS5's arrival time, the time between its formation and subsequent ejection, is $t_{\text{arr}} = 105 \pm 18(\text{stat}) \pm 30(\text{sys}) \text{ Myr}$.

This timescale provides an interesting new constraint on the origin of unbound runaways and HVSs. Runaway B stars near the disk have $t_{\text{arr}} = 0\text{--}30 \text{ Myr}$, consistent with disk ejection scenarios involving a supernova in a binary system or a dynamical event among several massive

stars. The set of B-type HVSs with known evolutionary states, on the other hand, have $t_{\text{arr}} = 50\text{--}100 \text{ Myr}$. This timescale is difficult to reconcile with any ejection mechanism requiring a massive star to attain unbound ejection. The central black hole ejection scenario, however, allows for any t_{arr} . Thus, the derived arrival times for HVSs support the black hole ejection model.

Future progress requires obtaining high resolution observations of other HVSs to constrain their age and distance. The age distribution of HVSs has important implications for the epochs of star formation and the growth of the central black hole (Bromley et al. 2012). Combined with future proper motion measurements, we hope to directly constrain the full space velocity and place of origin of the HVSs.

This work was supported in part by the Smithsonian Institution. J. Cohen acknowledges partial support from NSF grant AST-0908139. This research makes use of NASA's Astrophysics Data System Bibliographic Services. We are grateful to the many people who have worked to make the Keck Telescopes and their instruments a reality, and who operate and maintain these observatories. The authors wish to extend special thanks to those of Hawaiian ancestry on whose sacred mountain we are privileged to be guests. Without their generous hospitality, none of the observations presented herein would have been possible

REFERENCES

- Abt, H. A., Levato, H., & Grosso, M. 2002, *ApJ*, 573, 359
 Behr, B. B. 2003, *ApJS*, 149, 67
 Bonanos, A. Z., López-Morales, M., Hunter, I., & Ryans, R. S. I. 2008, *ApJ*, 675, L77
 Bromley, B. C., Kenyon, S. J., Geller, M. J., & Brown, W. R. 2012, *ApJ*, 749, L42
 Brown, W. R., Anderson, J., Gnedin, O. Y., et al. 2010, *ApJ*, 719, L23
 Brown, W. R., Geller, M. J., & Kenyon, S. J. 2012, *ApJ*, 751, 55
 Brown, W. R., Geller, M. J., Kenyon, S. J., & Kurtz, M. J. 2005, *ApJ*, 622, L33
 Castelli, F., Gratton, R. G., & Kurucz, R. L. 1997, *A&A*, 318, 841
 Castelli, F. & Kurucz, R. L. 2004, arXiv:astro-ph/0405087
 Chini, R., Hoffmeister, V. H., Nasserri, A., Stahl, O., & Zinnecker, H. 2012, *MNRAS*, accepted
 Edelmann, H., Napiwotzki, R., Heber, U., Christlieb, N., & Reimers, D. 2005, *ApJ*, 634, L181
 Ekström, S., Georgy, C., Eggenberger, P., et al. 2012, *A&A*, 537, A146
 Ghez, A. M., Salim, S., Weinberg, N. N., et al. 2008, *ApJ*, 689, 1044
 Gillessen, S., Eisenhauer, F., Trippe, S., et al. 2009, *ApJ*, 692, 1075
 Girardi, L., Bertelli, G., Bressan, A., et al. 2002, *A&A*, 391, 195
 Girardi, L., Grebel, E. K., Odenkirchen, M., & Chiosi, C. 2004, *A&A*, 422, 205
 Gnedin, O. Y., Brown, W. R., Geller, M. J., & Kenyon, S. J. 2010, *ApJ*, 720, L108
 Gray, R. O. & Corbally, C. J. 1994, *AJ*, 107, 742
 Gualandris, A. & Portegies Zwart, S. 2007, *MNRAS*, 376, L29
 Gvaramadze, V. V. 2009, *MNRAS*, 395, L85
 Gvaramadze, V. V., Gualandris, A., & Portegies Zwart, S. 2009, *MNRAS*, 396, 570
 Hanssen, B. M. S. 2007, *ApJ*, 671, L133
 Heber, U., Edelmann, H., Napiwotzki, R., Altmann, M., & Scholz, R.-D. 2008a, *A&A*, 483, L21
 Heber, U., Hirsch, H. A., Edelmann, H., et al. 2008b, in ASP Conf. Ser., Vol. 392, Hot Subdwarf Stars and Related Objects, ed. U. Heber, C. S. Jeffery, & R. Napiwotzki, 167
 Hills, J. G. 1988, *Nature*, 331, 687
 Huang, W. & Gies, D. R. 2006, *ApJ*, 648, 580
 Irrgang, A., Przybilla, N., Heber, U., Fernanda Nieva, M., & Schuh, S. 2010, *ApJ*, 711, 138
 Kenyon, S. J., Bromley, B. C., Geller, M. J., & Brown, W. R. 2008, *ApJ*, 680, 312
 Kurucz, R. L. 1993, *SYNTHES* Spectrum Synthesis Programs and Line Data (Kurucz CD-ROM; Cambridge, MA: Smithsonian Astrophysical Observatory)
 Löckmann, U. & Baumgardt, H. 2008, *MNRAS*, 384, 323
 López-Morales, M. & Bonanos, A. Z. 2008, *ApJ*, 685, L47
 Lu, J. R., Ghez, A. M., Hornstein, S. D., Morris, M. R., Becklin, E. E., & Matthews, K. 2009, *ApJ*, 690, 1463
 Madigan, A.-M., Hopman, C., & Levin, Y. 2011, *ApJ*, 738, 99
 Madigan, A.-M., Levin, Y., & Hopman, C. 2009, *ApJ*, 697, L44
 Merritt, D. & Poon, M. Y. 2004, *ApJ*, 606, 788
 Perets, H. B., Gualandris, A., Merritt, D., & Alexander, T. 2009, *ApJ*, 702, 884
 Perets, H. B., Hopman, C., & Alexander, T. 2007, *ApJ*, 656, 709
 Perets, H. B. & Subr, L. 2012, *ApJ*, 751, 133
 Portegies Zwart, S. F. 2000, *ApJ*, 544, 437
 Press, W. H., Teukolsky, S. A., Vetterling, W. T., & Flannery, B. P. 1992, *Numerical recipes in C. The art of scientific computing* (Cambridge: University Press, 2nd ed.)
 Przybilla, N., Nieva, M. F., Heber, U., & Butler, K. 2008a, *ApJ*, 684, L103
 Przybilla, N., Nieva, M. F., Heber, U., et al. 2008b, *A&A*, 480, L37
 Przybilla, N., Nieva, M. F., Tillich, A., et al. 2008c, *A&A*, 488, L51
 Przybilla, N., Tillich, A., Heber, U., & Scholz, R.-D. 2010, *ApJ*, 718, 37
 Silva, M. D. V. & Napiwotzki, R. 2011, *MNRAS*, 411, 2596
 Tillich, A., Heber, U., Geier, S., et al. 2011, *A&A*, 527, A137

Tillich, A., Przybilla, N., Scholz, R., & Heber, U. 2009, *A&A*, 507, L37

Vogt, S. S., Allen, S. L., Bigelow, B. C., et al. 1994, *Proc. SPIE*, 2198, 362

Wang, J. & Merritt, D. 2004, *ApJ*, 600, 149

Yu, Q. & Tremaine, S. 2003, *ApJ*, 599, 1129